Astron. Astrophys. 349, 825–833 (1999)

ASTRONOMY AND ASTROPHYSICS

Near-infrared photometry of the young open clusters NGC 1893 and Berkeley 86⋆

A. Vallenari[1], **A. Richichi**[2], **G. Carraro**[3], **and L. Girardi**[3]

[1] Padova Astronomical Observatory, Vicolo Osservatorio 5, I-35122 Padova, Italy (vallenari@pd.astro.it)
[2] Arcetri Astrophysical Observatory, Largo E. Fermi, I-50110 Firenze, Italy (richichi@arcetri.astro.it)
[3] Department of Astronomy, Padova University, Vicolo dell'Osservatorio 5, I-35122 Padova, Italy (carraro,lgirardi@pd.astro.it)

Received 23 March 1999 / Accepted 5 August 1999

Abstract. We present photometry in the J and K near-infrared bands for two regions centered on the young open clusters NGC 1893 and Berkeley 86. We study 700 stars down to K = 17 in the field of NGC 1893, and about 2000 stars in the field of Berkeley 86 down to K$\sim$ 16.5, for which near-infrared photometry was insofar not available. Coupling J-K data with UBV photometry taken from literature, we produce reddening corrected colour-magnitude diagrams. We find that our data are consistent with previous determinations: the clusters are roughly coeval with an age between 4 and 6 million years. The mean reddening (measured as E(J-K)) values turn out to be 0.35 and 0.50 for NGC 1893 and Berkeley 86, respectively.

Using colour-colour plots we discuss the presence of candidate pre-main sequence stars showing infrared excess. Candidates are found in both cluster regions, confirming the young age of these clusters.

Key words: techniques: photometric – Galaxy: open clusters and associations: general – Galaxy: open clusters and associations: individual: Berkeley 86 – Galaxy: open clusters and associations: individual: NGC 1893 – infrared: stars

1. Introduction

Open clusters and associations in the Galactic disk are the best tools to investigate the distribution of population inside the disk and the spiral arms. We have undertaken a project to obtain deep near-infrared photometry of Galactic open clusters, aimed at deriving age, age spread, reddening, distance. About 10 clusters have already been observed. In the first paper, the ages of the old open clusters Berkeley 18 and Berkeley 17 have been derived and compared with the age of the Galactic disk (Carraro et al. 1999). In this paper we present J and K photometry for two young open clusters: NGC 1893 and Berkeley 86, whose fundamental properties are listed in Table 1. Two forthcoming papers will discuss the age of King 5 and IC 166, NGC 7789 respectively.

Send offprint requests to: Antonella Vallenari (vallenari@pd.astro.it)

⋆ Based on observations taken at TIRGO

NGC 1893 is a very young cluster involved in the bright diffuse nebulosity IC 410, associated with two pennant nebulae, Shain and Gaze 129 and 130, and obscured by several conspicuous dust clouds.

UBV photometry of NGC 1893 has been carried out by Cuffey (1973) and Massey et al. (1995). More than 39 members are bright early spectral type stars, responsible for the photoionization of the IC 410 nebula.

Tapia et al. (1991, TCER hereafter) perform near-infrared and Strömgren photometry for 50 stars down to K = 12.00. They estimate the age of the cluster to be 4×10^6 yr, derive the distance modulus $(M-m)_0 = 13.18\pm0.11$, and the reddening A_v=1.68. Strömgren photometry for 50 stars in the field of NGC 1893 has also been reported by Fitzsimmons (1993), who confirms the distance and age found by TCER.

Berkeley 86 is another young open cluster, located inside the OB association Cyg OB 1, and obscured by a foreground dust cloud. Optical photometry was carried out by Forbes et al. (1992) in the UBV pass-bands, and in the UBVRI bands by Deeg & Ninkov (1996) and Massey et al. (1995). They find that the cluster has an age of 5×10^6 yr, is moderately reddened (E(B-V) $\approx$ 1.0) and has an initial mass function close to the Salpeter one. Berkeley 86 hosts the famous eclipsing binary system V444 Cygni.

Strömgren photometry has also been obtained by Delgado et al. (1997) down to V = 19, who derive a slightly older age (8.5×10^6 yr) and a distance modulus of $(M - m)_0 = 11.1$.

No infrared photometry exists for this cluster.

In this paper we present near-infrared photometry for these two clusters, down to the limiting magnitude of K $\sim$ 16.5–17.0. In Sect. 2 we detail the observations and data reduction process. In Sect. 3 and 4 we discuss in turn for NGC 1893 and Berkeley 86 clusters the derived colour-magnitude diagrams and the detection of pre-main sequence candidates. We summarizes our results in Sect. 5.

2. Observations and data reduction

J (1.2 μm) and K (2.2 μm) photometry of the two clusters was obtained with 1.5m Gornergrat Infrared Telescope (TIRGO) equipped with Arcetri Near Infrared Camera (ARNICA) in Oc-

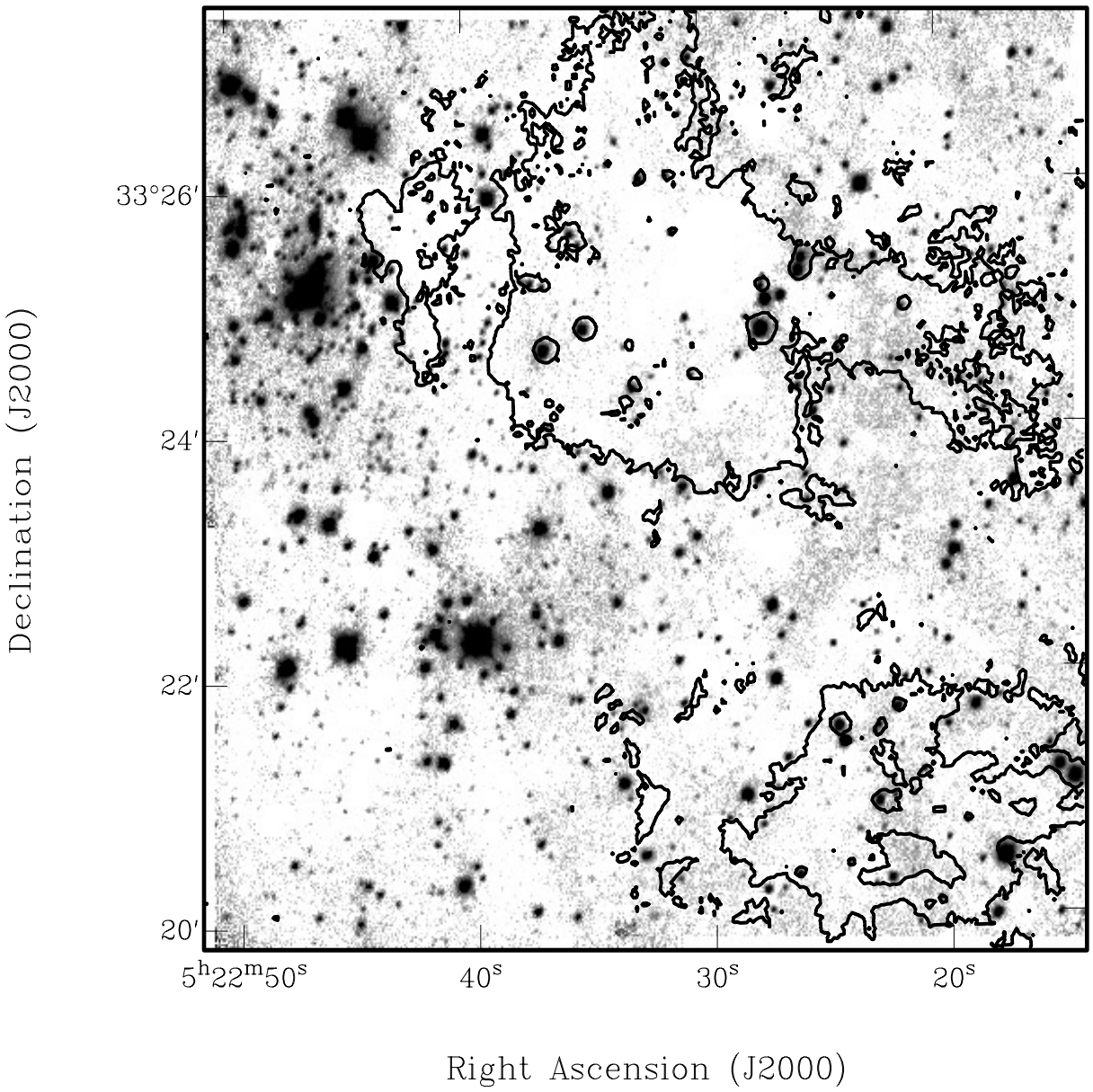

Fig. 1. Image in J band covering the studied region of NGC 1893. North is on the top, east at the left. The contours represent the dark clumps visible in the DSS image as explained in the text.

Table 1. Basic parameters of the studied clusters.

Cluster	l ^{o}	b ^{o}	Diameter ($\prime$)	Age Myr	A_V	$(M-m)_0$	Reference
NGC 1893	173.59	-1.70	13	4	1.68	13.18	Tapia et al. (1991)
Berkeley 86	76.66	1.26	6	5	3.1	11.1	Massey et al. (1995)
				8.5			Delgado et al. (1997)

tober 1997. ARNICA relies on a NICMOS3 256×256 pixel array (gain=20 e^-/ADU, read-out noise=50 e^- angular scale $=1''$/pixel, and $4' \times 4'$ field of view). Through each filter 4 partially overlapping images of each cluster were obtained, covering a total field of view of about $8\,' \times 8\,'$, in short exposures to avoid sky saturation. The observed field of NGC 1893 is covering approximately the SW quadrant of the region studied by Tapia et al. (1991). Only about $1/4$ of the total cluster area has been covered by our observations. The field was chosen to study the stellar content of the dark clumps in NGC 1893. The observed field of Berkeley 86 includes the vast majority of this cluster. Berkeley 86 was studied by Deeg & Ninkov (1996)

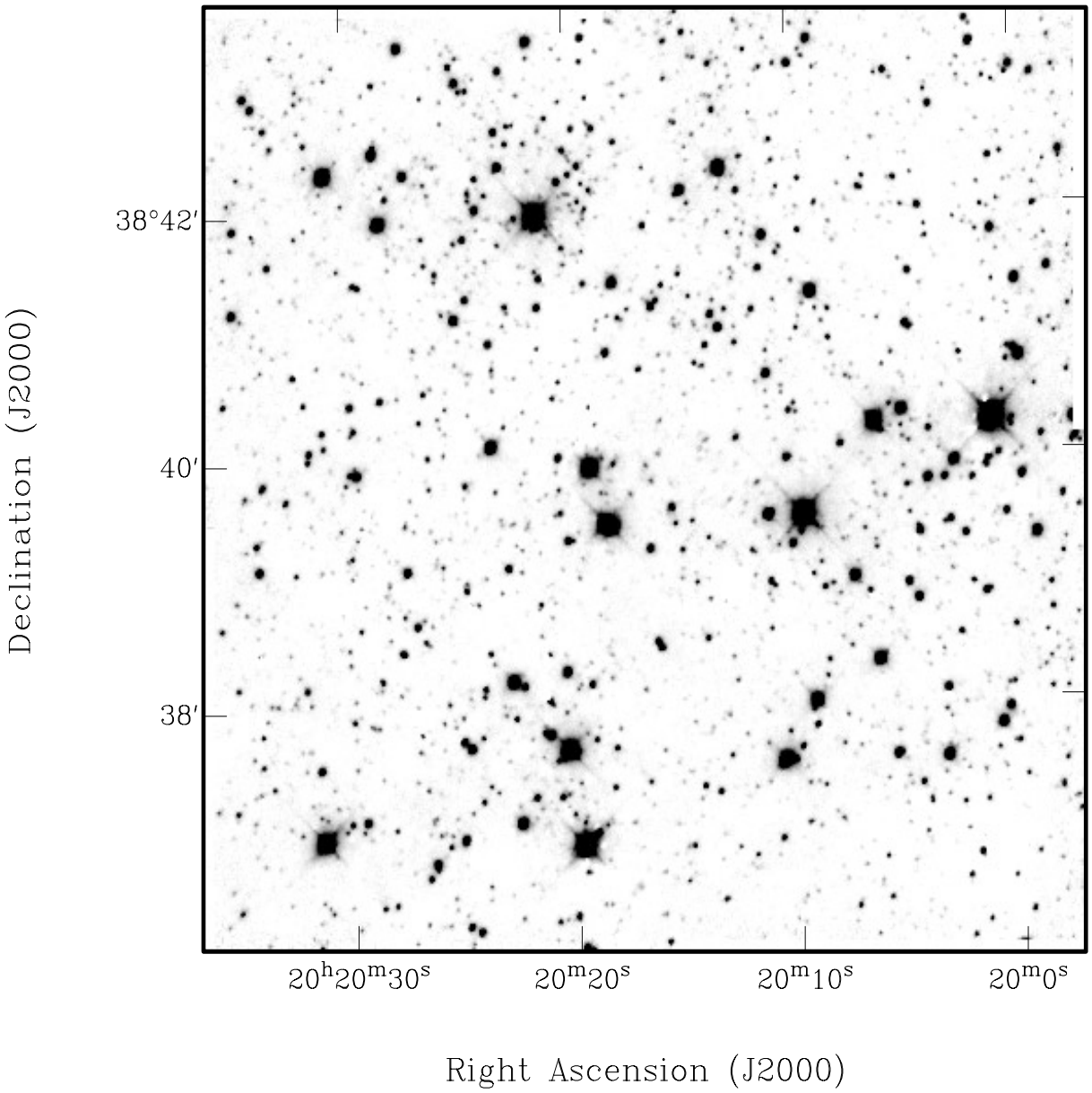

Fig. 2. Image in J band covering the studied region of Berkeley 86. North is on the top, east at the left.

who derive U,B,V,R,I photometry for stars in a slightly smaller field of $6' \times 6'$. The log-book of the observations is given in Table 2 were the total exposure times are given. The nights were photometric with a seeing of $1''$-$1.5''$. Figs. 1 and 2 present the mosaics of the 4 frames obtained per cluster in J passband.

The data are reduced subtracting from each image a linear combination of the corresponding skies and dividing the results by flat fields taken on twilight sky. We make use of the Arnica package (Hunt et al. 1994) in IRAF. Daophot II is used to perform photometry.

The conversion of the instrumental magnitude j and k to the standard J, K is made using stellar fields of standard stars taken by Hunt et al. (1998) list. We point out that the JHK Tirgo system is found by Hunt et al. (1998) to be consistent with the UKIRT system as described by Casali & Hawarden (1992). About 10 standard stars per night have been used. The relations per 1 sec exposure time are:

$$J = j + 19.51 \quad (1)$$

$$K = k + 18.94 \quad (2)$$

with standard deviation of the zero points of 0.03 mag for the J and 0.04 for the K magnitude. This error is only due to the linear interpolation of the standard stars. The calibration uncertainty is dominated by the error due to the correction from aperture photometry to PSF fitting magnitude. Taking it into account, we estimate that the total error on the calibration is about 0.1 mag both in J and K pass-bands. The standard stars used for the calibration do not cover the entire colour range of the data, because of the lack of stars redder than (J-K)~ 0.8. From our data, no colour term is found for K mag, whereas we cannot

Table 2. Observation Log-Book. The coordinates listed below refer to the center of the mosaic.

Cluster	α (2000)	δ (2000)	Date	Exposure Times (sec) J	K
NGC 1893	55 22 34	33 23 29	Oct, 22, 1997	720	660
Berkeley 86	20 20 18	38 39 27	Oct, 25, 1997	420	420
			Oct, 26, 1997	480	420

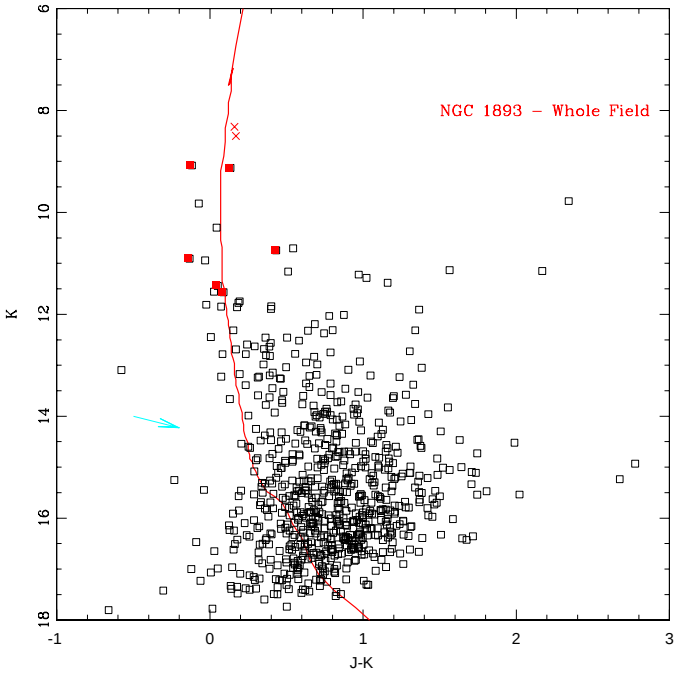

Fig. 3. The CMD of the whole observed region inside NGC 1893 with isochrone from Padova models having an age of 4 Myr and E(J-K)=0.35. The arrow indicates the reddening vector corresponding to E(J-K)=0.35. Solid squares indicate bona fide members on the basis of Tapia et al. spectroscopy. Crosses shows the bona fide members brighter than K=9 not included in our observed field taken from Tapia et al. photometry.

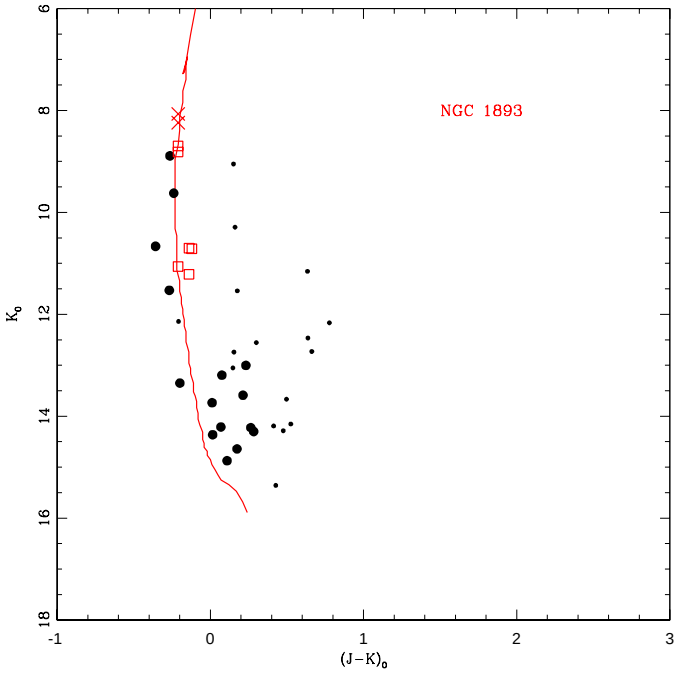

Fig. 4. De-reddened CMD for 38 stars in the field of NGC 1893, obtained as described in the text. An isochrone from Padova models having an age of 4 Myr is plotted. Solid circles represent candidate members, selected on the basis of the reddening. Open squares indicate bona fide members on the basis of Tapia et al. spectroscopy. Crosses show the bona fide members brighter than K=9 not included in our observed field taken from Tapia et al. photometry.

exclude it for the J magnitude. The limiting magnitudes are K $\sim$ 17 and 16.5 for NGC 1893 and Berkeley 86 respectively.

The data tables will be published electronically at the Centre des Donnes Stellaires of Strasbourg.

3. NGC 1893

3.1. The color-magnitude diagrams

The K-(J-K) CMD for NGC 1893 is shown in Fig. 3.

The cluster MS extends vertically between K=8–8.5 and 14, while at fainter magnitudes it is contaminated by field stars.

We compare our photometry with TCER one. Only 10 bright stars (down to K $\sim$ 13) in common are found.

The comparison between our photometry and TCER photometry gives:

$$K - K_{TCER} = 0.013, \quad \sigma = 0.07 \qquad (3)$$

$$(J-K) - (J-K)_{TCER} = 0.029, \quad \sigma = 0.08 \qquad (4)$$

To investigate whether this JK CMD is consistent with Tapia et al. cluster parameter determination, we assume their determination of reddening and distance and we over-impose on the CMD an isochrone (taken from Padova models, Bertelli et al. 1994, Girardi et al. 1999) of age of 4 million years (cf Fig. 3). Bona fide members brighter than K=9 located outside the observed field, but included in Tapia et al. photometry are also taken into account. A good agreement with the CMD is found. A de-reddened CMD will be presented and discussed in the following Section.

3.2. The extinction

Using the catalog of stars in the BV pass-bands in NGC 1893 given Massey et al. (1995) we identify about 57 stars brighter than V$\sim$ 18 (or K $\sim$ 14) in common with our study. From the (V-K)-(J-K) plot shown in Fig. 6 we derive the de-reddened CMD for all the 38 stars located at the right of the main sequence loci

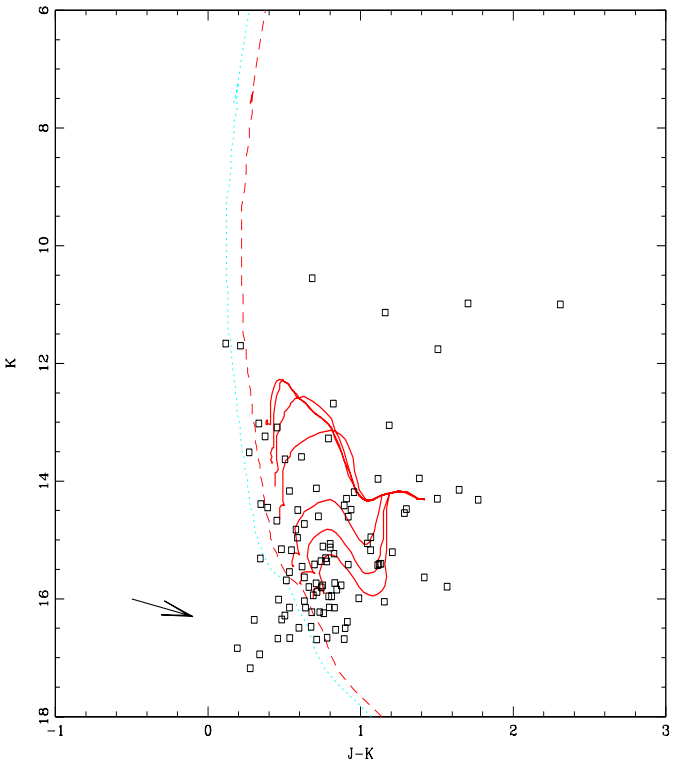

Fig. 5. CMD of the dark clump inside NGC 1893, as discussed in the text, selected on error on the magnitude $\sigma < 0.1$. Isochrones corresponding to an age of 4×10^6 yr, E(J-K)=0.55 and E(J-K)=0.45 (long dashed line and short dashed line respectively) are also shown, together with pre-main sequence tracks by Bernasconi with E(J-K)=0.55 for stellar masses 7,5,4,3,2,1.7,1.5 $M_\odot$ (solid lines). The arrow is the reddening vector for E(J-K)=0.4

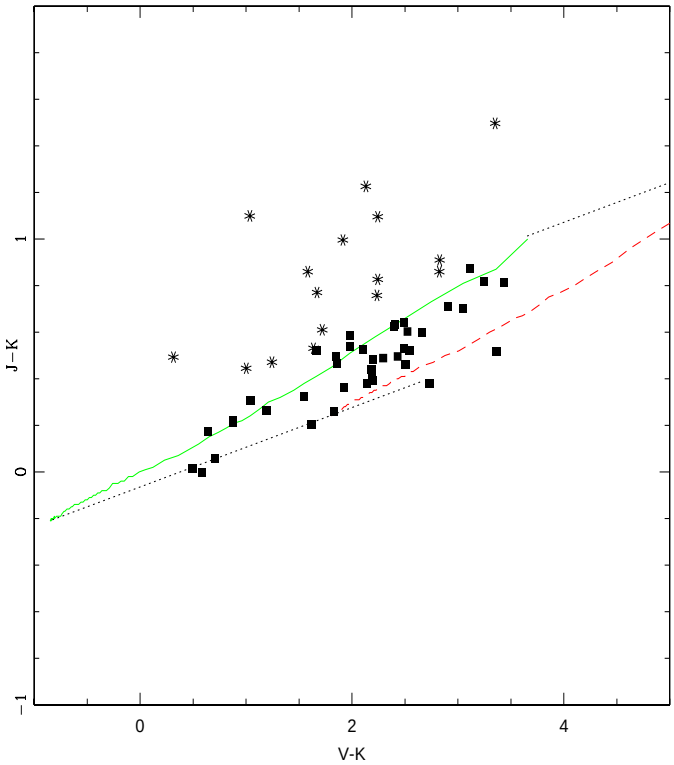

Fig. 6. (J-K)-(V-K) plot for 57 stars in NGC 1893. The lines show the loci of main sequence stars for E(J-K)=0 (solid line) and 0.65 (dashed line). The reddening vectors are indicated by dotted lines. Asterisks indicate objects suspected to be PMS candidates, as discussed in the text

(see discussion in Sect. 3.3). The resulting CMD is presented in Fig. 4. We find an E(J-K) ranging from 0.15 to 0.5 inside the whole region. This is in agreement with Massey et al. who find E(B-V) $\sim$ 0.4–0.7 (corresponding to E(J-K) $\sim$ 0.2–0.36) for the candidate members. Assuming their determination, we select, as candidate members, objects having E(J-K)= 0.2–0.4. The dereddened main sequence location is in reasonable agreement with a 4 Myr isochrone. We point out however, that selecting members on the basis of the reddening is probably not very effective in regions where gas and dust are present. The extinction is expected to be extremely variable.

The whole observed region is embedded in a large cloud associated to the cluster (Leisawitz et al. 1989) with CO emission. A comparison with a Digitized Sky Survey (DSS) image allows us to identify dark dusty clumps (see Fig. 1). We roughly define two main dark regions: $\alpha < 5^h22^m30^s$ and $\delta < 33^0 22'$ and $\alpha < 5^h22^m40^s$ and $\delta > 33^0 24'$. Fig. 5 presents the CMD of these dark clump regions where a 4×10^6 yr isochrone is plotted. While in the visual pass-bands these clumps are sparsely populated, in the JK CMD they appear to be populated by objects fainter than K $\sim$ 11. Isochrones fitting to the blue edge of the main sequence allows us to find the minimum reddening inside the region. We derive E(J-K) as high as 0.45–0.55 inside the dark clumps, slightly higher than the mean reddening derived outside the dark clumps.

We compare our determination of the reddening with the maps by Mendez & Van Altena (1998). They find at the distance of 4.3 Kpc, corresponding to the de-reddened distance modulus of 13.20, a value of E(B-V)=0.43$\pm$0.23 (or E(J-K)=0.26 $\pm$0.16), slightly lower than, but in reasonable agreement with the reddening given by NGC 1893.

3.3. Pre-main sequence candidates

Using BV photometry by Massey et al. (1995) we derive the J-(V-J) CMD presented in Fig. 8.

It is not possible to distinguish between pre-main sequence (PMS) stars and field contamination on the basis of the CMD. However, PMS stars often show infrared excesses due to the presence of circumstellar disks/envelopes. Emissions from dust and gas heated by either accretion or photospheric radiation or both, can be evidentiated by combining optical and near-IR photometry (see Hillenbrand et al. 1998). The idea is to select PMS candidates that populate the (V-K)-(J-K) and the (B-V)-(J-K) plots in a region forbidden to normally reddened stars.

Theoretical simulations (Calvet et al. 1991, Meyer et al. 1997, Hillenbrand et al. 1998) show that the effect of circumstellar disks/envelope on the magnitude of the resulting object

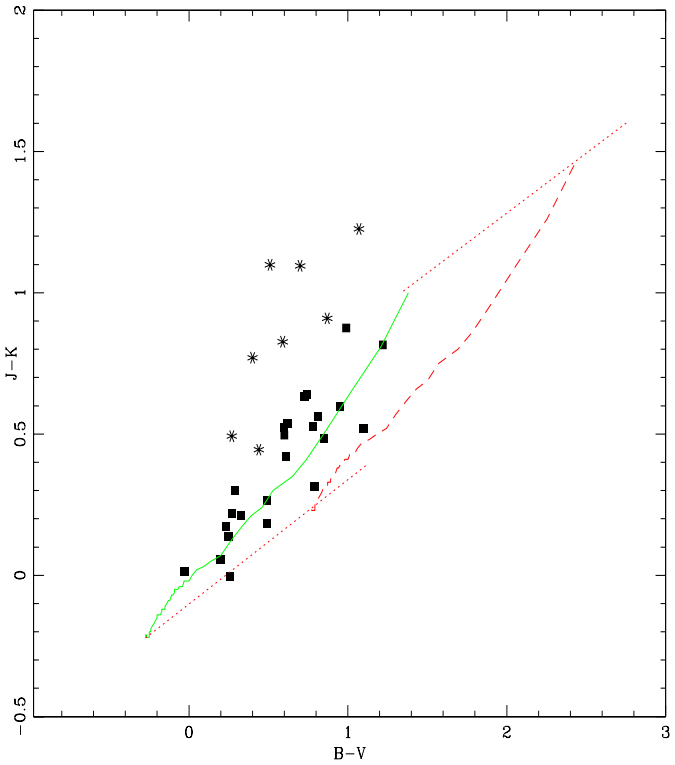

Fig. 7. (B-V)-(J-K) plot for 33 stars in NGC 1893. The lines show the loci of main sequence stars for E(J-K)=0 (solid line) and 0.65 (dashed line). The reddening vectors are indicated by dotted lines. Asterisks indicate objects suspected to be PMS candidates on the basis of Fig. 6 (see discussion in the text)

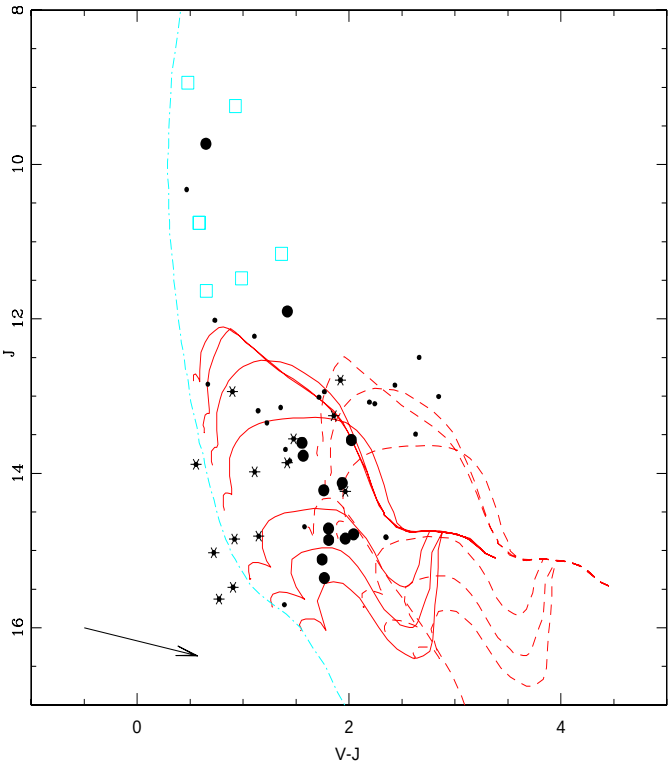

Fig. 8. J-(V-J) plot for 57 stars in NGC 1893. The dashed-dotted lines show 4 Myr isochrones having E(J-K)=0.2. The lines show the loci of PMS stars by Bernasconi (1996) having E(J-K)=0.2 (solid line) and 0.4 (dashed line) and masses 1.5,1.7,2,3,4,5,7 $M_{\odot}$. Open squares indicates main sequence stars of known membership from spectroscopy. Solid circles are suspected members derived from reddening analyis as described in the text. Asterisks show objects having infrared excess. The arrow indicates the reddening vector corresponding to E(J-K)=0.2.

is maximum in the K band, slightly lower in the J band. B and V colours instead can be considered as purely photospheric, unless an accretion disk is present. In this case, also these latter filters can be affected by a blue excess due to the hot accretion zone (Hartigan et al. 1991). We note that we were not able to apply corrections for reddening for PMS candidates while using this method, since there are no reliable determination of the reddening for these stars. Moreover, the reddening changes quite unpredictably inside the field of view.

Fig. 6 presents the (J-K)-(V-K) diagram for 57 stars in NGC 1893. For 33 of them B magnitudes are available, the corresponding (B-V)-(J-K) diagram is shown Fig. 7. 16 stars are found outside the reddening vectors in the (J-K)-(V-K) plot. To be very conservative, only stars located 0.1 outside the reddening vectors are considered as candidates. Only 8 of them have B known magnitudes and they are located in the (B-V)-(J-K) plot in the region forbidden to normally reddened stars. They can be regarded as pre-main sequence candidates. The location of pre-main sequence stars in the colour-colour diagrams adopted for this method obviously depend on several parameters, including the size and geometry of the disk/envelope, the physical properties of the dust grains, the characteristics of the central star and more. Therefore, the method cannot be used to assess in detail the characteristics of the PMS candidates, but only to draw some global conclusions on statistical basis. Hillebrand et al. (1998) find that the efficiency of the colour-colour plots to detect PMS T Tauri and Herbig Ae/Be stars depends on the adopted colour plot, but is not higher than 70%. Additionally, we note that this method only applies to PMS candidates with a surrounding dust disk or envelope, and will miss all the so-called naked (or weak-line) T Tauri stars. It is not completely clear whether these latter represent an evolutionary phase or an independent phenomenon, but we know that depending on the star-forming region their incidence can be quite important even at ages of a few million years (for instance, in the Taurus-Auriga complex). Therefore, we conclude that a fortiori our estimate of the number of PMS candidates in NGC 1893 is a lower limit.

From the Log T-Log L plane PMS tracks by Bernasconi (1996) we calculate the BVJK magnitudes, using the tables of corrections by Bertelli et al. (1994). The comparison with the observations in the J-(V-J) plane (cf Fig. 8) suggests that the majority of the stars having IR-excess can be PMS objects located close to a reddened 4 Myr isochrone (E(J-K) $\sim$ 0.2–0.4) and having 2–4 and possibly 7 $M_{\odot}$ masses. If all the stars inside NGC 1893 are born at the same time, we expect that objects more massive than 2–3 $M_{\odot}$ have already reached the main sequence. Indeed, a star having 7 $M_{\odot}$ mass needs about 6.3 $\times 10^5$ to reach the main sequence, and a 4 $M_{\odot}$ mass star needs 1.5

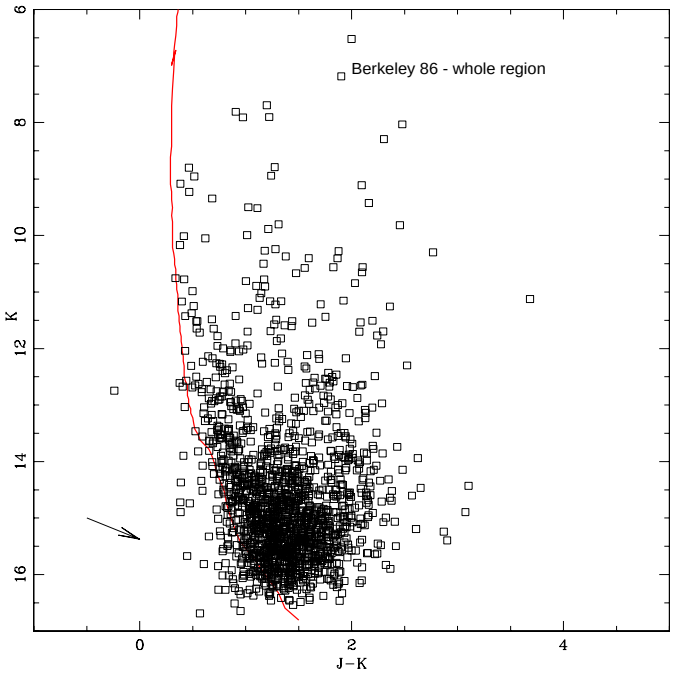

Fig. 9. CMD of Berkeley 86 (whole region) with isochrone from Padova models having an age of 6 Myr and E(J-K)=0.5. The arrow indicates the reddening vector corresponding to E(J-K)=0.5

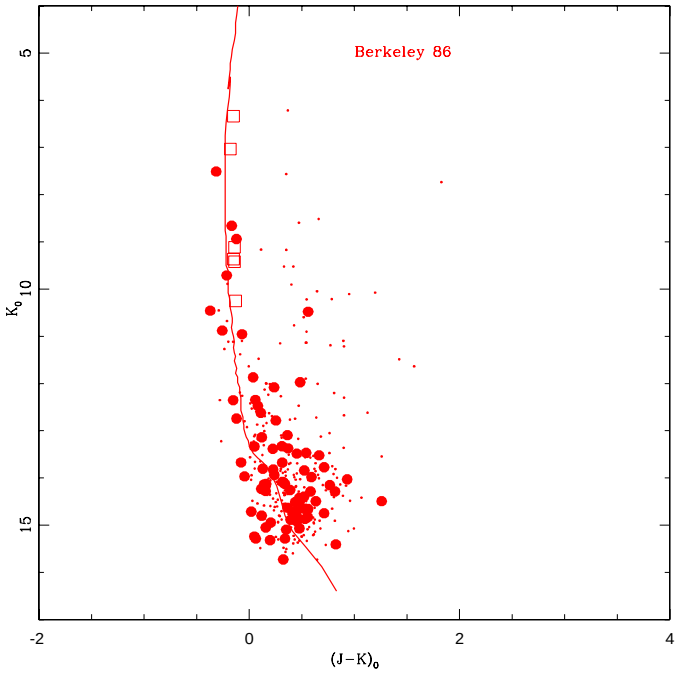

Fig. 10. Reddening corrected CMD of Berkeley 86 with an isochrone from Padova models having an age of 6 Myr. Solid circles indicate suspected members, selected on the basis of the reddening, open squares represent members known from spectroscopy (Massey et al. 1995).

$\times 10^6$ yr. If these candidates are true PMS stars a large spread in age might be present. However, since in these passbands the reddening vector is almost parallel to the x-axis, differential reddening can be responsible for the location of these intermediate mass PMS candidates in the CMD. It cannot be excluded that some of the PMS candidates belong to the field population. Additionally, when combining optical and near-infrared photometry which have not been obtained simultaneously, the expected strong variability of the sources might affect the results. Definitive identification of accreting systems can be obtained only by mean of spectroscopic determination.

As we discussed in the previous section, an optically obscured clump with CO emission is located inside the observed field. Such a region might be the birthplace of young objects. A comparison of the CMD of this region with PMS tracks by Bernasconi (see Fig. 5) suggests that at least some of the detected stars can be PMS candidates. Since almost no stars inside this region have BV photometry, the method of the colour-colour plot to detect PMS candidates cannot be applied.

4. Berkeley 86

4.1. The CMD

The CMD of the observed region inside Berkeley 86 is shown in Fig. 9. The contamination from interlopers is very high. However it is possible to distinguish a vertical MS. With a distance modulus of $(m-M)_o$=11.1 (Massey et al. 1995) an isochrone of 6 Myr and E(J-K)=0.5 seems to reproduce the main sequence location.

We identify about 340 stars in common with Deeg & Ninkov (1996) photometry for which UBVRI magnitudes are available. Using their estimate of the E(B-V) for each stars we derive the corresponding E(J-K), following the relation E(J-K)/E(B-V)=0.52 (Cardelli et al. 1989). The final K-(J-K) CMD reddening corrected is presented in Fig. 10. E(J-K) is found ranging from 0.45 to 0.64. The relative frequency of objects inside the field with the E(J-K) is peaked at E(J-K) $\sim$ 0.5. The suspected members are selected on the basis of the reddening, E(J-K) ranging from 0.48 to 0.52, roughly corresponding to 1 σ in the color excess distribution. As in the case of NGC 1893 we point out that a selection of the members on the basis of the reddening gives only a rough indication in regions where dust and gas are present, since the extinction might be highly variable.

The reddening maps by Mendez & van Altena (1998) give E(B-V)=0.96 or E(J-K) $\sim$ 0.41 at the distance of 1700 pc, where Berkeley 86 is located. The maximum expected reddening inside the region is E(B-V)=2.3 or E(J-K)=0.99. This is in good agreement with our determinations, considering that the mean error on the Mendez & van Altena maps is about δ E(J-K)=0.16.

4.2. Pre-main sequence candidates

Coupling Deeg & Ninkov photometry with our JK magnitudes, we discuss the presence of candidate pre-main sequence stars. Since I magnitudes are available, we make use of the (V-I)-(I-K) plot. Hillenbrand et al. have shown that this color combination is specially effective in identifying stars with infrared excess. Fig. 11 presents the (V-I)-(I-K) plot for the stars in com-

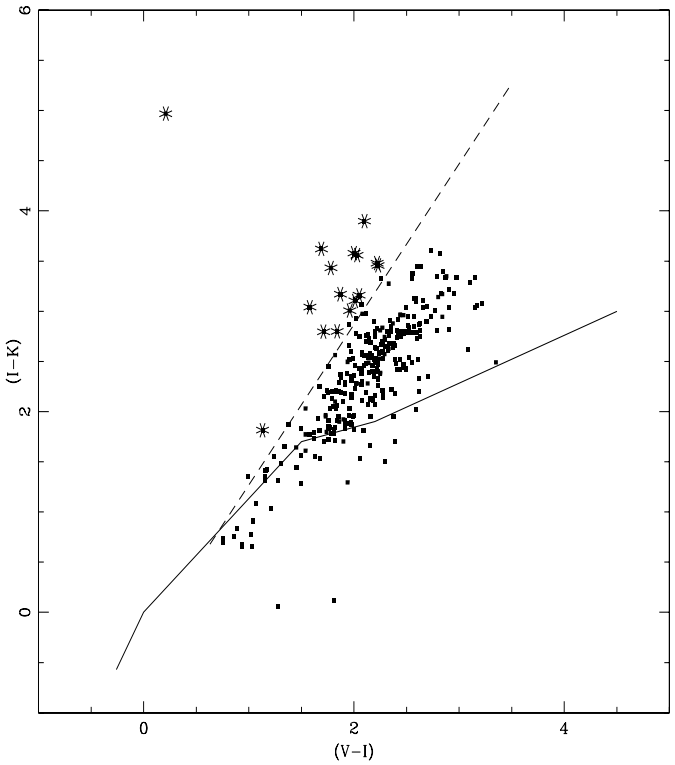

Fig. 11. (V-I)-(I-K) plot for about 340 stars in Berkeley 86. The solid line give the loci of the main sequence and giant stars having reddening E(J-K)=0. Reddening vector is indicated by a dashed line. Asterisks show the candidate pre-main sequence stars.

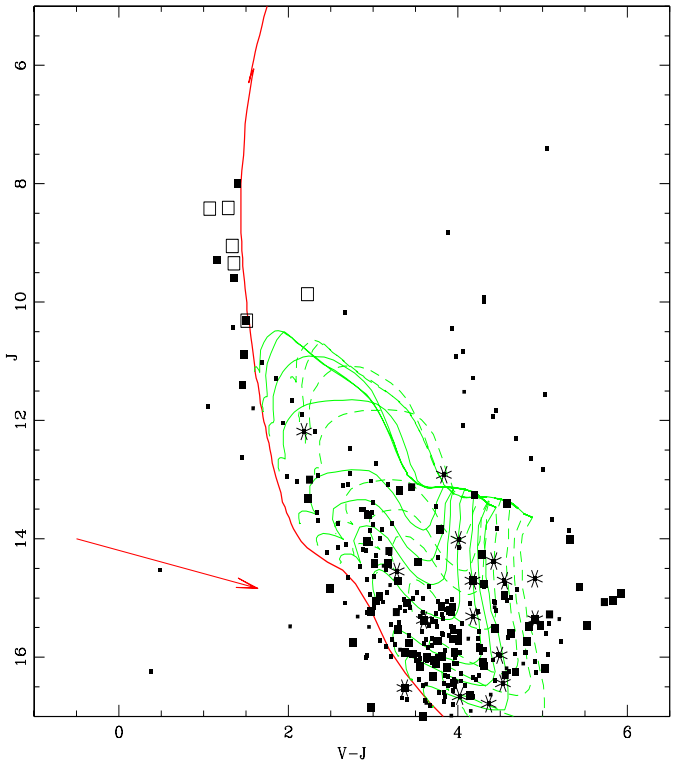

Fig. 12. J-(V-J) plot for about 340 stars in Berkeley 86. The stark solid line represents a 6 Myr isochrone having E(J-K)=0.5. Stars indicate pre-main sequence candidates. Open squares show members known from spectroscopy. Solid squares present suspected members selected on the basis of the reddening (see text). Dashed lines are pre-main sequence tracks by Bernasconi, for masses 0.8,0.9,1.0,1.2,1.5,1.7,2,3,4,5,7 and reddening E(J-K)= 0.6 and solid lines are the analogous for E(J-K)= 0.5. The arrow is the reddening vector corresponding to E(J-K)= 0.5.

mon with Deeg & Ninkov (1996). 16 stars seem to be good pre-main sequence candidates. In Fig. 12 their location in the J-(V-J) CMD is presented. A comparison with the pre-main sequence tracks shows that the majority of these candidates might have low masses, between 1.7 and 0.8 $M_{\odot}$. Only two candidates are found in the region occupied by higher mass stars. We cannot exclude however that these stars belong to the background population. Since the time a 1.7 $M_{\odot}$ star need to reach the main sequence is longer than the age of Berkeley 86 (about 1.5 $\times 10^7$ yr, Bernasconi 1996) no need of a large age spread is found inside the population of Berkeley 86.

5. Conclusions

We have presented J and K near-infrared photometry down to a limiting magnitude of K $\sim$17 and 16.5 for the two very young, highly obscured open clusters NGC 1893 and Berkeley 86, respectively. For Berkeley 86 near-infrared photometry was not available before our study, while in the case of NGC 1893 previous near-infrared photometric survey only reached K=13. We confirm previous determinations of the age, distance and reddening of these clusters. Coupling J-K data with Johnson photometry we discuss the presence of stars with IR excess, as pre-main sequence candidates. Several good candidates are identified in both clusters, confirming the young age of these objects. Spectroscopic measurements are requested to definitively identify pre-main sequence objects.

Acknowledgements. The authors are thankful to the referee C. Dougados for many useful comments. This research has been sponsored by the Italian Ministry of University and Research, and by the Italian Space Agency.

References

Bernasconi P.A., 1996, A&AS 120, 57
Bertelli G., Bressan A., Chiosi C., Fagotto F., Nasi E., 1994, A&AS 106, 275
Calvet N., Patino A., Magris G.C., D'Alessio P., 1991, ApJ 380, 617
Casali M.M., Hawarden T.G., 1992, JCMT-UKIRT Newsletter N 4, 33
Cardelli J.A., Calyton G.C., Mathis J.S., 1989, ApJ 345, 245
Carraro G., Vallenari A., Girardi L., Richichi A., 1999, A&A 343, 825
Cuffey J., 1973, AJ 78, 747
Deeg H.J., Ninkov Z., 1996, A&AS 119, 221
Delgado, A.J., Alfaro, E.J., Cabrera-Caño J., 1997, AJ 113, 713
Fitzsimmons A., 1993, A&AS 99, 15
Forbes D., English E., De Roberts M.M., Dawson P.C., 1992, AJ 103, 916
Girardi L., Bressan A., Bertelli G., Chiosi C., 1999, in preparation
Hillenbrand L.A., Strom S.E., Calvet N., et al., 1998, AJ 116, 1861
Hartigan P., Kenyon S.J., Hartmann L., et al., 1991, ApJ 382, 617
Hunt L.K., Mannucci F., Testi L., et al., 1998, AJ 115, 2594

Hunt L., Testi L., Borelli S., Maiolino, R., Moriondo G., 1994, Arcetry Observatory Technical Report N.4/94
Leisawitz D., Bash F.N., Thaddeus P., 1989, ApJS 70,731
Massey P., Johnson K.E., DeGioia-Eastwood K., 1995, ApJ 454, 151
Meyer M.R., Calvet N., Hillenbrand L.A., 1997, AJ 114, 288
Mendez R., van Altena 1998, A&A 330, 910
Tapia M., Costero R., Echevarría J., Roth M., 1991, MNRAS 253, 649